Article

Optimization of Giant Magnetoimpedance Effect of Amorphous Microwires by Postprocessing

Valentina Zhukova [1,2,3], Paula Corte-Leon [1,2,3,4], Ahmed Talaat [1,2,3], Mihail Ipatov [1,2], Alfonso García-Gomez [1,2,3], Alvaro González [1,2,3], Juan Maria Blanco [2,3] and Arcady Zhukov [1,2,3,5,*]

[1] Department Polymers and Advanced Materials: Physics, Chemistry and Technology, Faculty of Chemistry, University of Basque Country, UPV/EHU, 20018 San Sebastian, Spain; valentina.zhukova@ehu.eus (V.Z.); paula.corte@ehu.eus (P.C.-L.); ahmed.talaatfarag@ehu.eus (A.T.); mihail.ipatov@ehu.es (M.I.); alfonso.garciag@ehu.eus (A.G.-G.); alvaro.gonzalezv@ehu.eus (A.G.)
[2] Department Applied Physics I, Escuela de Ingeniería de Gipuzkoa EIG, University of Basque Country, UPV/EHU, Plaza Europa 1, 20018 San Sebastian, Spain; juanmaria.blanco@ehu.es
[3] EHU Quantum Center, University of the Basque Country, UPV/EHU, 20018 San Sebastian, Spain
[4] Department of Materials Science & Metallurgy, University of Cambridge, 27 Charles Babbage Road, Cambridge CB3 0FS, UK
[5] IKERBASQUE, Basque Foundation for Science, 48011 Bilbao, Spain
* Correspondence: arkadi.joukov@ehu.es; Tel.: +34-94-301-8611; Fax: +34-94-301-7130

Abstract: Magnetic microwires with amorphous structures can present a unique combination of excellent magnetic softness and giant magnetoimpedance (GMI) effects together with reduced dimensions and good mechanical properties. Such unique properties make them suitable for various technological applications. The high GMI effect, observed in as-prepared Co-rich microwires, can be further optimized by postprocessing. However, unexpected magnetic hardening and a transformation of the linear hysteresis loop into a rectangular loop with a coercivity on the order of 90 A/m were observed in several Co-rich microwires upon conventional annealing. Several routes to improve magnetic softness and GMI effect in Fe- and Co-rich magnetic microwires are provided. We observed that stress annealing could remarkably improve the magnetic softness and GMI ratio of Co-rich microwires. Thus, almost unhysteretic loops with a coercivity of 2 A/m and a magnetic anisotropy field of about 70 A/m are achieved in Co-rich microwires stress annealed at appropriate conditions. The observed change in hysteresis loops and the GMI effect is explained by stress-annealing-induced anisotropy, which is affected by the stresses applied during annealing and by the annealing temperature. While as-prepared Fe-rich amorphous microwires present a low GMI effect, appropriate postprocessing (annealing and stress annealing) allows for a remarkable GMI ratio improvement (an order of magnitude). The evaluated dependence of the maximum GMI ratio on frequency allows the identification of the optimal frequency band for the studied samples. The origin of stress-annealing-induced anisotropy and related changes in hysteresis loops and the GMI effect are discussed in terms of the relaxation of internal stresses, "back-stresses", as well as structural anisotropy.

Keywords: magnetic microwires; magnetic anisotropy; magnetoimpedance effect; hysteresis loops; internal stresses; induced magnetic anisotropy

1. Introduction

Unusual magnetic properties, such as ultrafast domain-wall propagation intrinsically related to magnetic bistability [1–4] and/or giant magnetoimpedance (GMI), an effect linked to excellent magnetic softness [5–9], make amorphous magnetic wires attractive for the development of several technological applications [10–15]. The above-mentioned GMI effect consists of a substantial change in the impedance, Z, of a magnetic conductor under the influence of an applied DC magnetic field [5–9]. Accordingly, studies of magnetic

properties and the GMI effect of amorphous magnetic wires have attracted substantial attention for several decades [10,16].

It is worth noting that generally amorphous materials present not only excellent magnetic properties (magnetic bistability, fast domain-wall propagation, extremely low coercivity, or GMI effect) but also superior mechanical properties [17,18], making them attractive for various emerging applications, such as magnetoelastic sensors or smart composites [14,19,20]. Additionally, amorphous materials usually have better corrosion properties [21].

The application possibilities can be considerably extended if the above-mentioned properties (corrosion and mechanical properties) are further improved. As demonstrated elsewhere [18], better mechanical properties can be obtained in materials with lower dimensions. Additionally, functional coatings (e.g., insulating glass) can also improve the corrosion properties and even the mechanical properties of fragile crystalline magnetic wires [10,22].

Therefore, studies of amorphous magnetic wires with reduced diameters have become relevant over the last three decades [9,10,16].

Among the most effective solutions for the preparation of thin amorphous magnetic wires coated with functional coating is the so-called Taylor–Ulitovsky technique, allowing the manufacturing of magnetic microwires covered with flexible, insulating, and biocompatible glass coating [10,23]. The presence of glass-coating (required by the fabrication process) allows the possibility of reducing the diameter of the metallic nucleus diameter of such glass-coated microwires up to 100 nm [24]. However, glass-coated microwires with amorphous structures can be obtained with diameters up to 100 μm [25]. In fact, the Taylor–Ulitovsky fabrication method was developed years ago principally for the fabrication of non-magnetic glass-coated microwires [26], and the preparation of amorphous glass-coated microwires was reported in the 1970s [27].

The perfectly cylindrical geometry of metallic nuclei in glass-coated microwires is especially beneficial for the realization of such unique magnetic properties as spontaneous magnetic bistability [3,4] or the GMI effect [9,10].

The GMI effect is intrinsically related to the magnetic softness of magnetic materials and consists of a large change in the impedance, Z, of a magnetically soft conductor under the action of an applied magnetic field [5–7]. Usually, the GMI effect is expressed as the GMI ratio, $\Delta Z/Z$, given as [5–7]

$$\Delta Z/Z = [Z(H) - Z(H_{max})]/Z(H_{max}) \cdot 100 \tag{1}$$

where H represents the given DC magnetic field, and H_{max} represents the maximum applied DC magnetic field (typically about a few kA/m).

In the case of Co-rich magnetic wires, $\Delta Z/Z$ values typically of 200–300% are reported [5–7]. However, in carefully processed magnetic microwires, $\Delta Z/Z$ values up to 650% have been achieved [9,10,28,29]. Typically, such changes in impedance appear upon rather low applied magnetic fields (below 10 kA/m).

Accordingly, the GMI effect is characterized by quite a high (up to 10%/A/m) magnetic field sensitivity, η, given as

$$\eta = \frac{\partial\left(\frac{\Delta Z}{Z}\right)}{\partial H} \tag{2}$$

Such η values, reported for the GMI effect in properly processed magnetic microwires, are among the largest observed for non-cryogenic effects.

The aforementioned high GMI effect is related to an extremely high impedance sensitivity to external stimuli, like magnetic fields, or even to applied stress. Elevated $\Delta Z/Z$ and η values are suitable for the development of high-performance magnetic field sensors and magnetometers [11–13].

Such advanced features of amorphous wires with GMI effect permitted the development of high-performance sensors suitable for monitoring of biomagnetic fields with pico-Tesla sensitivity [11,13].

The GMI effect origin is satisfactorily explained in terms of the variation in the skin depth, Δ, of an *AC* electrical current flowing through a magnetically soft conductor under an applied magnetic field, H [5–9]. Such strong Δ variation upon applying a magnetic field in a soft magnetic conductor is attributed to the high circumferential magnetic permeability, μ_ϕ, of magnetic wires. The relationship between Δ and μ_ϕ is given by [5,9]

$$\Delta = \frac{1}{\sqrt{\pi \sigma \, \mu_\Phi f}} \tag{3}$$

where σ represents the electrical conductivity, and f represents the AC electric current frequency.

Therefore, the GMI effect can be observed in magnetic materials with high magnetic permeability and good magnetic softness, the main prerequisite for a high GMI effect [5–9].

The magnetic softness of amorphous materials is commonly attributed to a liquid-like structure characterized by the absence of defects typically found in crystalline materials (dislocations, grain boundaries, and twin boundaries). However, there are several sources of magnetic anisotropy, such as magnetoelastic anisotropy, surface irregularities, or short-range ordering (clusters, interstitial impurities, pair ordering, internal stresses, etc.), that can affect the magnetic softness of amorphous materials [30,31]. Accordingly, a generally better magnetic softness is reported for amorphous materials with vanishing magnetostriction coefficient, λ_s [32–34]. Such nearly-zero λ_s values can be observed for Co-rich compositions, particularly in Co_xFe_{1-x} or Co_xMn_{1-x} alloys with $0.03 \leq x \leq 0.08$ [32–35].

The other source of the magnetoelastic anisotropy of amorphous materials is the internal stresses arising during the fabrication process [9,10]. In amorphous wires, the main source of internal stresses is associated with the fabrication process involving rapid melt quenching [31,32,36]. However, in glass-coated microwires, the contribution of internal stresses induced by different thermal expansion coefficients of the metallic alloy and the glass is even higher [10,23,37]. Such internal stresses have a complex character, with the highest axial component within the main part of the metallic nucleus [23,37]. Such character of internal stresses, together with compositional λ_s dependence, results in a strong axial magnetic anisotropy in Fe-rich glass-coated microwires with high and positive λ_s values (up to 40×10^{-6}). Therefore, as-prepared Fe-rich microwires usually present a rectangular character of hysteresis loops with relatively low μ_ϕ values and, hence, a low GMI effect [38]. However, Co is relatively expensive and even belongs to critical raw materials [39].

As mentioned above, up to now, the highest $\Delta Z/Z$ values of up to 650% have been achieved in carefully processed magnetic microwires [9,10,28,29]. However, achieved $\Delta Z/Z$ values are substantially below the theoretically predicted $\Delta Z/Z \approx 3000\%$ [7,9]. The performance of sensors and devices based on the GMI effect can be significantly improved by using materials with a higher GMI effect. Therefore, certain attention has been paid to studies of postprocessing to allow magnetic softness and GMI effect improvement in less expensive Fe-based microwires [10,38]. On the other hand, there are several successful attempts to improve magnetic softness and GMI effect even in Co-rich microwires [40].

Consequently, in this paper, we provide an overview of the routes allowing optimization of the magnetic softness and GMI effect in Fe- and Co-rich glass-coated amorphous microwires.

2. Materials and Methods

We prepared several Fe-, Fe-Co-, and Fe-Co-Ni-based glass-coated microwires with either positive or vanishing magnetostriction coefficients, λ_s, using the Taylor–Ulitovsky preparation method described in detail elsewhere [9,10,23,37].

Briefly, the fabrication procedure consists of melting a pre-prepared metallic alloy (typically of a few grams) with a high-frequency inductor (often 350–500 kHz) inside

a Pyrex-like glass tube. After that, a capillary is formed from the softened glass tube, which is captured by a rotating receiving spool [10,23,37]. The molten metallic alloy then fills the glass capillary, forming a microwire with a metallic nucleus fully covered with a continuous, thin, and flexible glass coating. A stream of coolant is used to achieve a high enough quenching rate of a composite metallic microwire covered with an insulating glass coating [10].

The hysteresis loops have been measured using the fluxmetric technique, previously described elsewhere [40]. This experimental technique was previously successfully employed for the characterization of magnetically soft microwires [40]. The studied samples were magnetized along the axial direction by 120 mm long and thin (8 mm in diameter) magnetization coil, producing a homogeneous magnetic field, H. For a better comparison of samples with different chemical compositions, the hysteresis loops were represented as the dependencies of normalized magnetization M/M_o on H (where M_o represents the magnetic moment of the samples at maximum amplitude H_o of magnetic field).

The dependencies of microwire impedance, Z, and GMI ratio, $\Delta Z/Z$ (defined by Equation (1)) on the applied magnetic field have been measured using a specially designed microstrip sample holder placed inside a sufficiently long solenoid allowing the creation of a homogeneous magnetic field, H. The sample impedance, Z, was measured using a vector network analyzer from the reflection coefficient S_{11} as described elsewhere [41]. The use of such a technique allowed us to measure $\Delta Z/Z(H)$ dependencies in the frequency range up to the GHz range [41].

The magnetostriction coefficients, λ_s, of the samples have been measured using the small-angle magnetization rotation (SAMR) method, recently adapted for measurements of magnetic microwires [34].

The compositions, geometrical parameters, and λ_s values of studied samples are provided in Table 1.

Table 1. Compositions and geometries of studied glass-coated microwires.

Composition	Metallic Nucleus Diameter, d (μm)	Total Diameter, D (μm)	Ratio $\rho = d/D$	Magnetostriction Coefficient, $\lambda_s \times 10^{-6}$
$Fe_{75}B_9Si_{12}C_4$	15.2	17.2	0.88	38
$Fe_{65}Si_{15}B_{15}C_5$	12.6	20	0.63	38
$Fe_8Co_{51}Ni_{18}B_{13}Si_{10}$	12.8	15.8	0.81	−0.3
$Co_{69.2}Fe_{3.6}Ni_1B_{12.5}Si_{11}C_{1.2}Mo_{1.5}$	22.8	23.2	0.98	−1
$Co_{67}Fe_{3.85}Ni_{1.45}B_{11.5}Si_{14.5}Mo_{1.7}$	16.8	24	0.7	−3
$Co_{67}Fe_{3.85}Ni_{1.45}B_{11.5}Si_{14.5}Mo_{1.7}$	25.6	26.6	0.96	−0.3

The morphologies of the studied microwires and the d and D values of the studied glass-coated microwires have been evaluated using an optical microscope Axio Scope A1. Several examples are provided in Figure 1. From the provided images of the studied microwires (see Figure 1a–c), rather homogeneous microwire geometries can be clearly appreciated, and the d and D values can be confirmed.

We studied the magnetic properties and the GMI effect of as-prepared and annealed microwires. The crystallization of amorphous microwires is generally observed at temperatures above 500 °C [10,22,25]. Therefore, to maintain amorphous structure, all thermal treatments have been performed at temperatures, T_{ann}, below 450 °C. The X-ray Diffraction (XRD) performed using a BRUKER (D8 Advance) X-ray diffractometer (Karlsruhe, Germany) with Cu Kα (λ_{XRD} = 1.54 Å) radiation was used for structural control of as-prepared and annealed microwires. As can be appreciated from Figure 2, wide halos typical for amorphous materials are observed in XRD spectra for as-prepared and for annealed at 400 °C samples (an example for $Co_{67}Fe_{3.85}Ni_{1.45}B_{11.5}Si_{14.5}Mo_{1.7}$ microwire is provided in Figure 2).
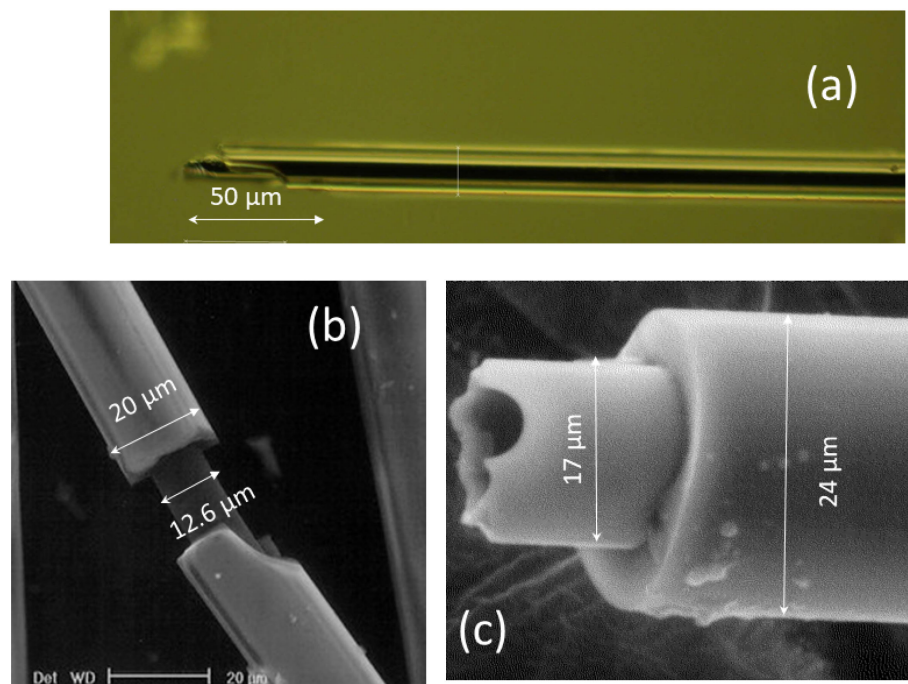
Figure 1. Optical microscopy images of $Fe_{75}B_9Si_{12}C_4$ (**a**), $Fe_{65}Si_{15}B_{15}C_5$ (**b**), and $Co_{67}Fe_{3.85}Ni_{1.45}B_{11.5}Si_{14.5}Mo_{1.7}$ (**c**) microwires. (**a**) is reproduced with permission from Ref. [42].
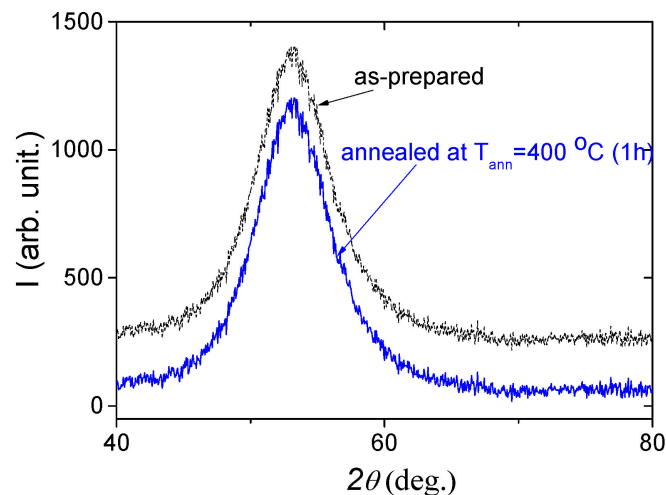
Figure 2. XRD patterns of as-prepared and annealed at 400 °C for 1 h $Co_{67}Fe_{3.85}Ni_{1.45}B_{11.5}Si_{14.5}Mo_{1.7}$ sample. Reproduced with permission from Ref. [42].

The existence of the insulating glass coating makes it possible to anneal the samples in air.

3. Experimental Results and Discussion

As can be seen in Figure 3, the hysteresis loops of as-prepared Fe-and Co-rich microwires are rather different. The rectangular hysteresis loop can be appreciated for Fe-rich microwires (see Figure 3a). Clearly, better magnetic softness is observed for the as-prepared Co-rich microwires (see Figure 3b). Therefore, the GMI performance of as-prepared Co-rich microwires is substantially better than that of Fe-rich microwires: a rather higher GMI ratio (at 200 MHz) is evidenced from Figure 1c for Co-rich microwires.
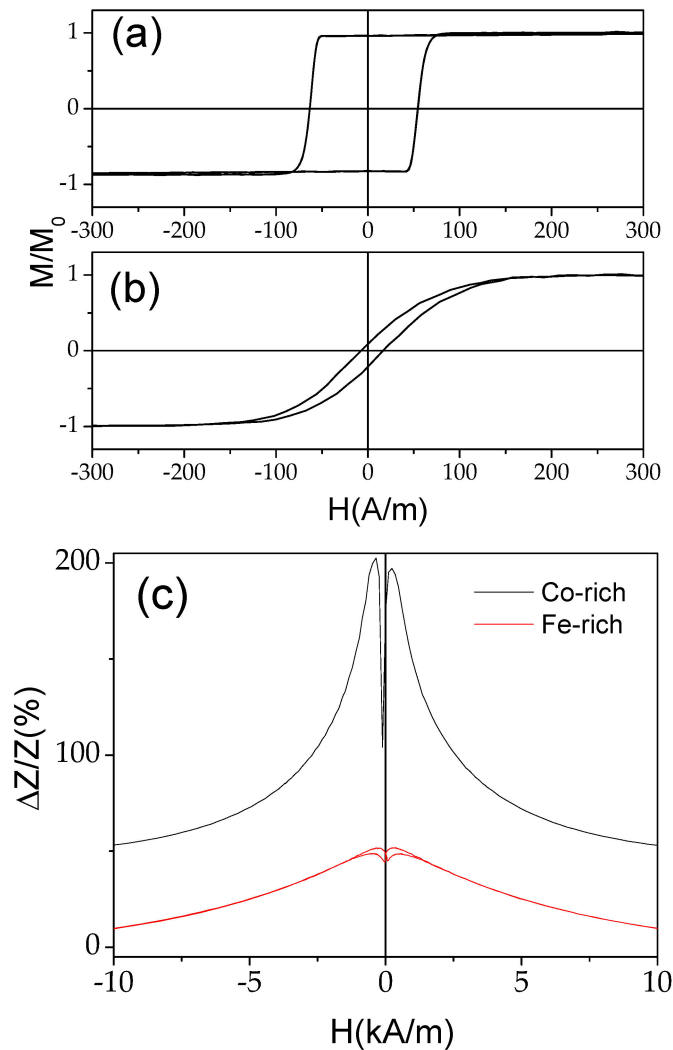
Figure 3. Hysteresis loops of $Co_{67.1}Fe_{3.8}Ni_{1.4}Si_{14.5}B_{11.5}Mo_{1.7}$ (d = 16.8 μm) (**a**) and $Fe_{70}B_{15}Si_{10}C_5$ (d = 12.6 μm) amorphous microwires (**b**) and $\Delta Z/Z(H)$ dependencies of as-prepared samples measured at 200 MHz (**c**).

It is worth noting that, somehow, a better magnetic softness and a slightly higher GMI effect can be observed in Fe-Ni-based microwires with lower λ_s values [10,42].

However, from the provided comparison, it is clear that as-prepared Fe-rich microwires are not attractive for GMI effect applications due to a rather low GMI effect. Therefore, further postprocessing is required for Fe-based microwires to be considered for GMI effect applications.

3.1. Routes of Magnetic Softnening and GMI Effect Optimization in Fe-Rich Amorphous Microwires

Below, we provide several experimental results on the effect of postprocessing on the magnetic properties and the GMI effect of amorphous Fe-rich microwires with a rather typical composition ($Fe_{75}B_9Si_{12}C_4$) and with large and positive λ_s (38×10^{-6}). However, similar behavior is observed for a variety of Fe-rich and Fe-Ni-rich microwires with positive λ_s, such as Fe74B13Si11C2 or Fe72B13Si11Nb3Ni1 [10,42].

Conventional furnace annealing at 300 and 400 °C only slightly affected the hysteresis loops of $Fe_{75}B_9Si_{12}C_4$ microwires (see Figure 4): a slight decrease in coercivity, H_c, is observed upon annealing. However, the overall rectangular shape of hysteresis loops remains unchanged.
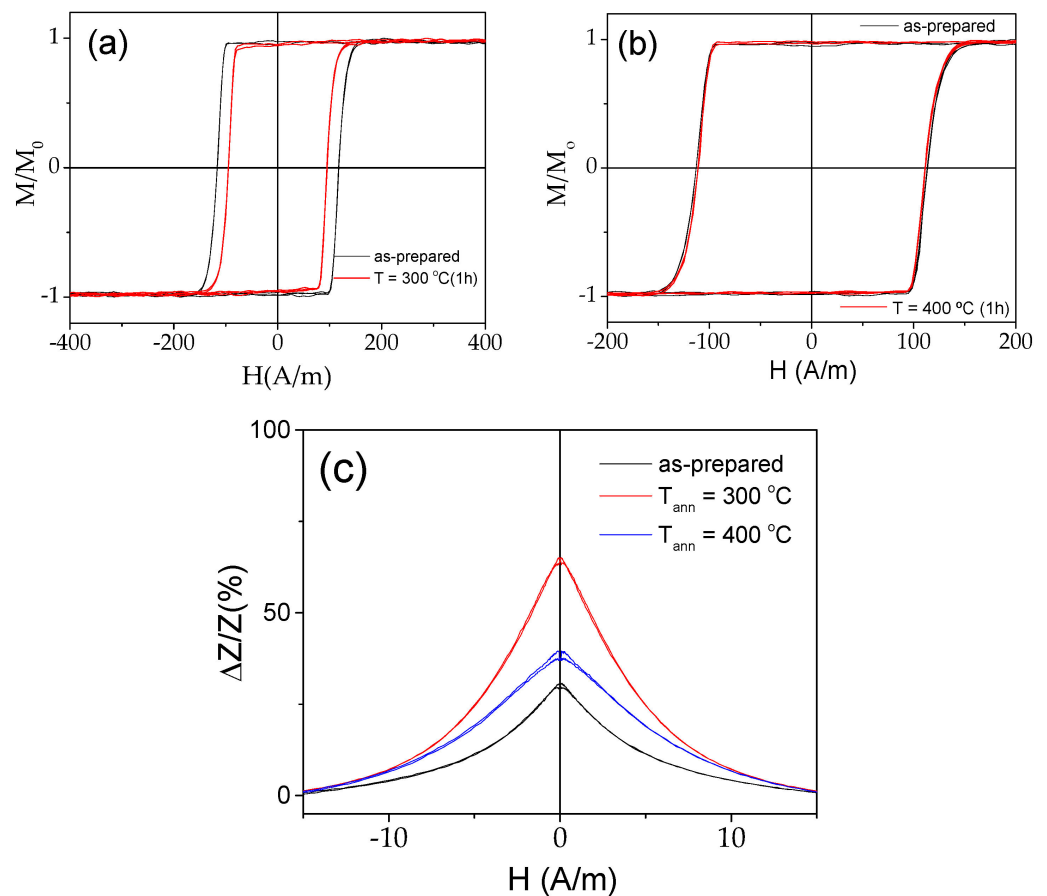
Figure 4. Effect of annealing at 300 °C (**a**) and 400 °C (**b**) on hysteresis loops of $Fe_{75}B_9Si_{12}C_4$ microwire and on GMI effect measured at 100 MHz (**c**).

Despite only a slight change in the hysteresis loops, even conventional annealing allows GMI effect improvement, as observed in Figure 4c.

As discussed elsewhere, the GMI effect value and the $\Delta Z/Z(H)$ dependence are intrinsically related to the magnetic anisotropy character. Among the factors that can contribute to the GMI effect improvement after annealing are internal stress relaxation and, hence, a lower axial magnetic anisotropy after annealing.

Recently, we demonstrated that remarkable transverse magnetic anisotropy can be induced in Fe-rich microwires by annealing under tensile stress: stress annealing allows effective tuning of the magnetic anisotropy [43,44]. Such stress-annealing-induced anisotropy depends on T_{ann}, tensile stress, σ_a, applied during the annealing. The modification of the hysteresis loops of $Fe_{75}B_9Si_{12}C_4$ microwire upon stress annealing is shown in Figure 5.

In both cases, shown in Figure 5, a transformation of perfectly rectangular hysteresis loops into inclined and almost linear with reduced coercivity is observed. Such transformation of hysteresis loops results in a substantial decrease in coercivity, H_c (see Figure 5c,d). Accordingly, such substantial stress-annealing-induced magnetic anisotropy and magnetic softening results in considerable improvement in the GMI ratio (see Figure 6). As can be observed in Figure 6a,b, maximum $\Delta Z/Z$ values, $\Delta Z/Z_{max}$, above 100% can be observed in stress-annealed Fe-rich microwires. However, some of the observed $\Delta Z/Z(H)$ dependencies are rather unusual. Thus, at intermediate frequencies, f (100–200 MHz), the $\Delta Z/Z(H)$ dependencies have irregular shapes.
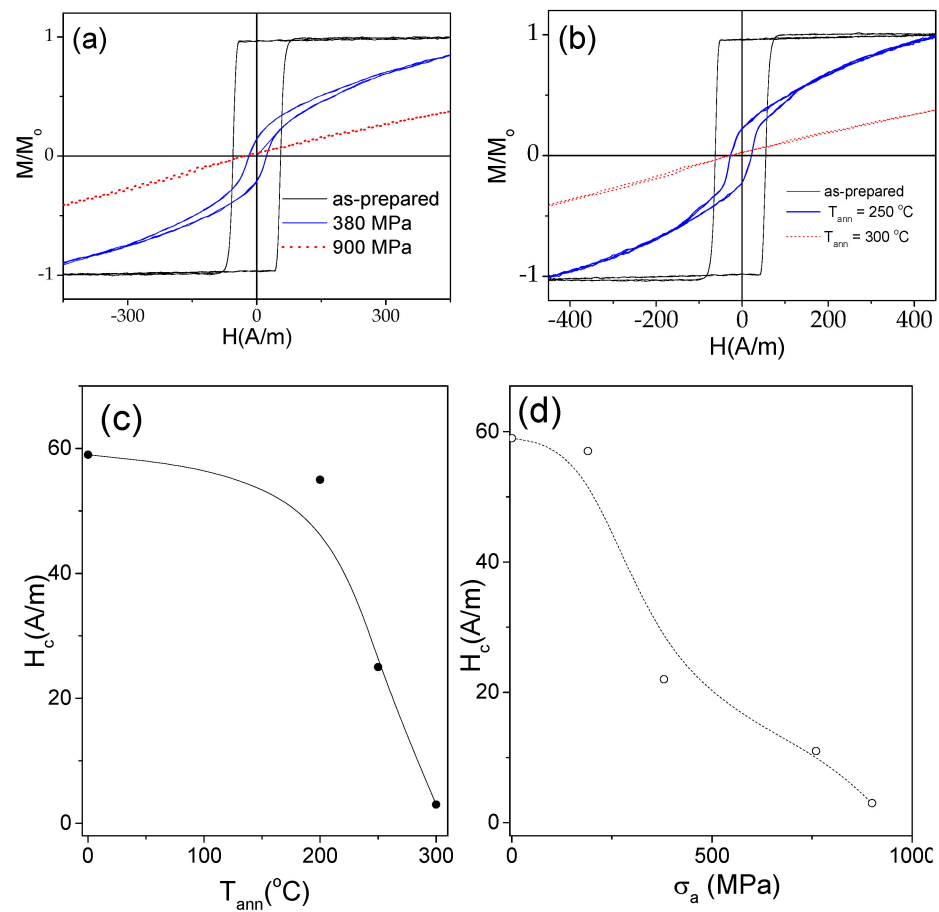
Figure 5. Effect of stress annealing at 300 °C at different σ$_a$ (**a**) and σ$_a$ = 900 MPa and T$_{ann}$ = 250 °C and 300 °C (**b**) on hysteresis loops of Fe$_{75}$B$_9$Si$_{12}$C$_4$ microwire and evolution of H_c versus T$_{ann}$ at σ$_a$ = 900 MPa (**c**) and H_c versus σ$_a$ at T$_{ann}$ = 300 °C (**d**).
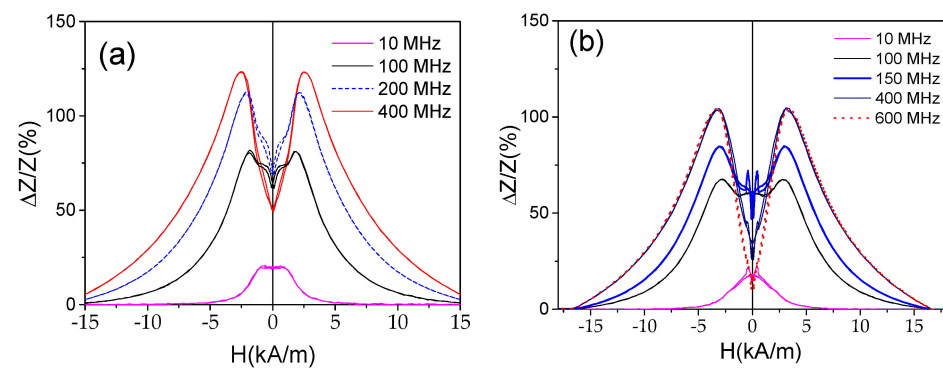
Figure 6. $\Delta Z/Z(H)$ dependencies of Fe$_{75}$B$_9$Si$_{12}$C$_4$ microwire stress annealed at T_{ann} = 250 °C (σ$_a$ = 900 MPa) (**a**) and T_{ann} = 300 °C (σ$_a$ = 900 MPa) (**b**) measured at different f.

From the definition of the magnetic field sensitivity, η, given by Equation (2), it is clear that the η magnitude correlates with $\Delta Z/Z_{max}$ value: for a given magnetic field interval η is higher for the samples with higher $\Delta Z/Z_{max}$. Accordingly, $\Delta Z/Z_{max}$ is an important factor from the viewpoint of application.

A comparison of $\Delta Z/Z(H)$ dependencies measured at low (f = 10 MHz) and high (f > 400 MHz) frequencies gives an idea that such irregular dependence is the superposition of roughly single peak $\Delta Z/Z(H)$ dependencies observed at low f and double-peak $\Delta Z/Z(H)$ dependencies observed at sufficiently high f (f > 400 MHz) [44]. Considering Equation (3),

it was assumed that such irregular $\Delta Z/Z(H)$ dependencies must be attributed to the contribution of the inner axially magnetized core, which should have a single-peak $\Delta Z/Z(H)$ dependence, and of the outer shell with a transverse magnetic anisotropy and a double-peak $\Delta Z/Z(H)$ dependence [44]. Increasing the frequency, the skin depth, Δ, decreases (see Equation(3)), and the contribution of the inner axially magnetized core gradually decreases as well. As mentioned above, the features of the shape of the $\Delta Z/Z(H)$ dependencies are determined by the magnetic anisotropy of magnetic wires: double-peak dependencies are predicted and experimentally reported for magnetic wires with circumferential magnetic anisotropy [5,6], whereas single-peak $\Delta Z/Z(H)$ dependencies (similar to those observed in Figure 4c) are typically observed for wires with axial magnetic anisotropy.

The GMI effect in stress-annealed Fe-rich amorphous microwires is explained in terms of core–shell magnetic structure, assuming the existence of the inner core with an axial magnetic anisotropy and external outer domain shell with a helical anisotropy [8,45–48].

The obtained $\Delta Z/Z_{max}$ values are reasonably high for magnetic sensor applications. The results provided above on the dependence of the GMI effect and the magnetic softening on postprocessing show that appropriate thermal treatment allows for the extension of Fe-rich microwires into GMI-related applications.

3.2. Tailoring of the GMI Effect and the Magnetic Softness in Co-Rich Microwires

As shown in Figure 3b,c, excellent magnetic softness and a high GMI effect can be achieved in as-prepared Co-rich microwires with a vanishing magnetostriction coefficient. In several cases, quite a high GMI ratio has been reported, even in as-prepared Co-rich microwires [28,49]. However, proper postprocessing can be useful for substantial GMI effect improvement [29,30].

Traditional heat treatment (furnace annealing), in most cases, is not suitable for magnetic softening and GMI effect improvement in Co-rich microwires. As shown below, considerable magnetic hardening is observed upon annealing of various Co-rich microwires (see Figures 7 and 8). Similar results have been reported for a variety of Co-rich microwires [10,49].
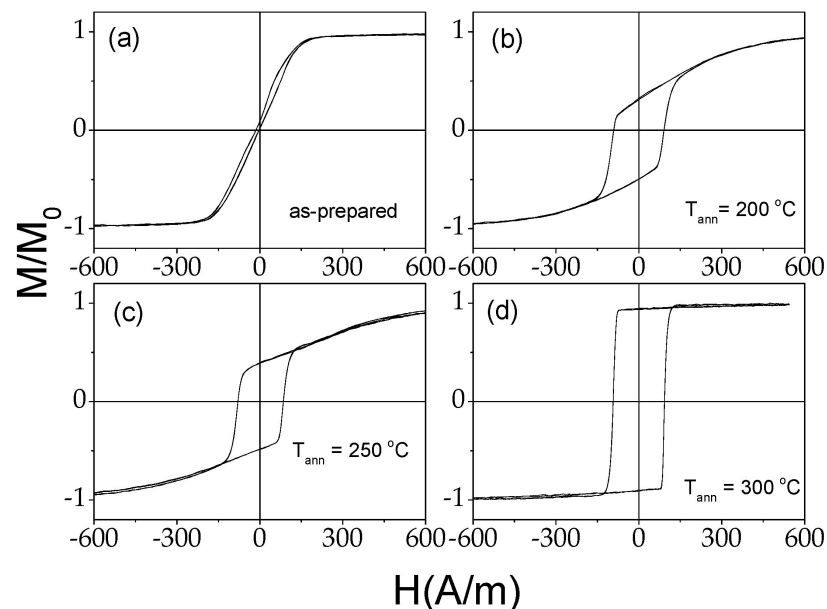

Figure 7. Hysteresis loops of $Fe_{3.6}Co_{69.2}Ni_1B_{12.5}Si_{11}Mo_{1.5}C_{1.2}$ microwires: as-prepared (**a**); and annealed at different T_{ann} for 60 min with σ_a = 900 MPa, T_{ann} = 200 °C (**b**), T_{ann} = 250 °C (**c**), and 300 °C (**d**).
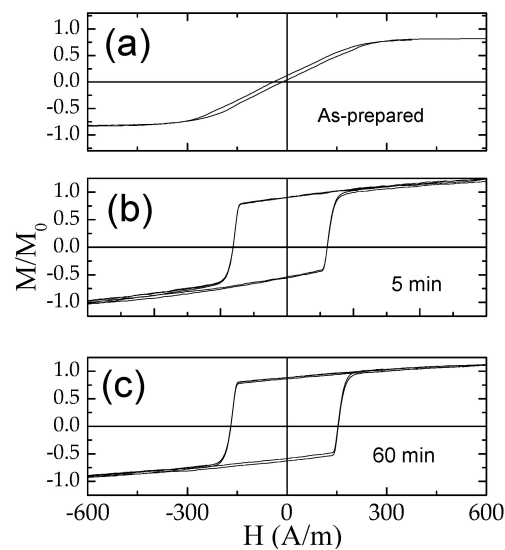
Figure 8. Effect of annealing time on hysteresis loops of $Fe_8Co_{51}Ni_{18}B_{13}Si_{10}$ microwires: as-prepared (**a**) and annealed at T_{ann} = 300 °C for 5 min (**b**) and 60 min (**c**). Reproduced with permission from Ref. [50].

Upon annealing, the hysteresis loop transformation from linear with quite a low coercivity, H_c, (typically below 10 A/m) into rectangular with almost an order of magnitude higher H_c values is observed. Accordingly, not only an increase in coercivity but also an increase in remanent magnetization, M_r/M_o, is observed.

As mentioned previously, the domain structure of magnetic wires is commonly described as consisting of an inner axially magnetized core and an outer shell with a transverse magnetization orientation [1,2,8,47,48,50–52]. As mentioned elsewhere [2,47,50,51], in the frame of such a model, the volume of the inner axially magnetized core can be evaluated from the M_r/M_o values as follows:

$$R_C = R\sqrt{\frac{M_r}{M_o}} \qquad (4)$$

where R_c and R are the inner core and the microwire radius, respectively.

As can be observed from Figures 7 and 8, both H_c and M_r/M_0 rapidly increase upon stress annealing, rising either with annealing time, t (at fixed T_{ann}), or annealing temperature, T_{ann} (at fixed t). Consequently, we must assume that the observed change in hysteresis loops consists of a substantial increase in the axially magnetized core radius, R_c, upon annealing. The dependencies of both H_c and M_r/M_0 on annealing conditions (t and T_{ann}) are summarized in Figure 9.

Such unexpected magnetic hardening of Co-rich microwires has been previously discussed in terms of stress-dependence of the magnetostriction coefficient previously reported for amorphous materials [42,53]. It was assumed, and even confirmed experimentally, that the internal stress relaxation produces changes in the λ_s value and even the sign (for small and negative λ_s) [42,51].

In terms of magnetic softening, the annealing of Co-rich microwires does not look appropriate. Additionally, in most cases, the GMI performance of annealed Co-rich microwires either remains similar to as-prepared samples or becomes even worse (see Figure 10). It must be noted that after annealing, in most of the cases, double-peak $\Delta Z/Z(H)$ dependencies transform into single peak (see Figure 10a,c) or at least the magnetic field of maximum $\Delta Z/Z$, H_m, becomes lower (see Figure 10b). Such changes in $\Delta Z/Z(H)$ dependencies are in agreement with the transformation of the hysteresis loops of Co-rich microwires shown in Figures 7 and 8. As mentioned above, single-peak $\Delta Z/Z(H)$ dependencies are typical for magnetic wires with axial magnetic anisotropy.
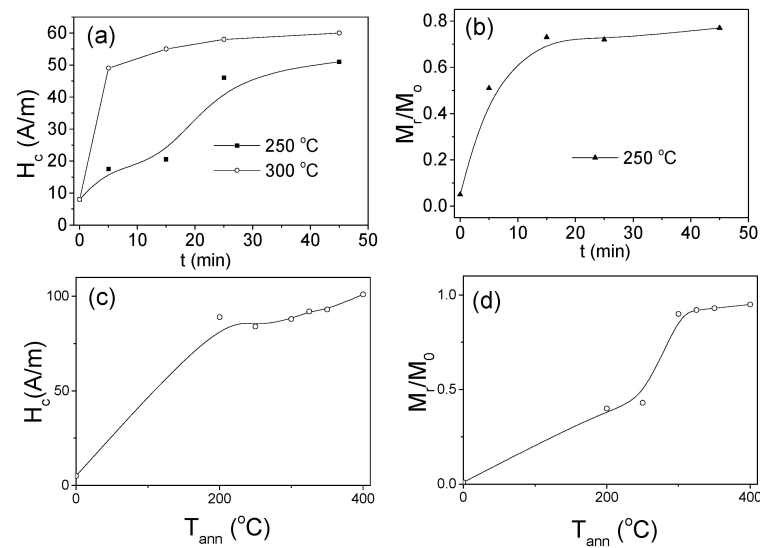
Figure 9. Dependence of coercivity, H_c, (**a**) and reduced remanent magnetization, M_r/M_o (**b**) on annealing time, t in $Co_{69.2}Fe_{4.1}B_{11.8}Si_{13.8}C_{1.1}$ microwires and dependence of coercivity, H_c, (**c**) and reduced remanent magnetization, M_r/M_o (**d**) on annealing temperature, T_{ann}, for $Fe_{3.6}Co_{69.2}Ni_1B_{12.5}Si_{11}Mo_{1.5}C_{1.2}$ microwires.
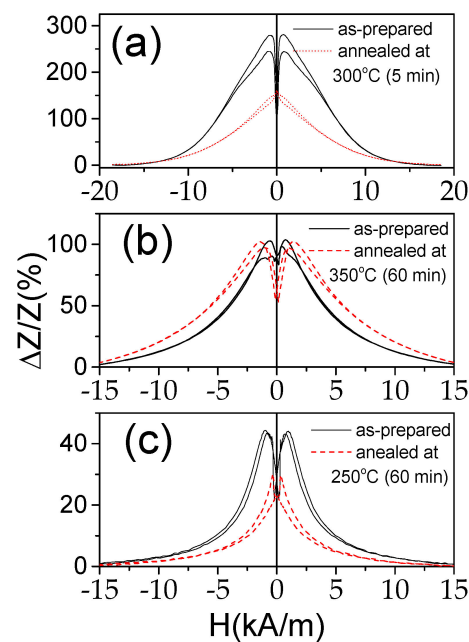

Figure 10. Effect of annealing at different conditions (T_{ann}, t_{ann}) on $\Delta Z/Z(H)$ dependencies of $Co_{69.2}Fe_{4.1}B_{11.8}Si_{13.8}C_{1.1}$ (**a**), $Co_{69.2}Fe_{3.6}Ni_1B_{12.5}Si_{11}C_{1.2}Mo_{1.5}$ (**b**), and $Fe_8Co_{51}Ni_{18}B_{13}Si_{10}$ (**c**) microwires measured at $f = 100$ MHz.

However, in such Co-rich microwires with magnetic bistability induced by annealing, $\Delta Z/Z_{max}$ values are still reasonably high. Similarly to Fe-rich microwires, the remagnetization process of Co-rich microwires with annealing-induced magnetic bistability runs through the single domain-wall propagation [50,51]. Therefore, such "universal" microwires presenting both of the most technologically interesting properties, such as ultrafast domain-wall propagation and a high GMI effect, can be useful for several technological applications [54].

Considering the successful use of stress annealing to induce transverse magnetic anisotropy in Fe-rich microwires, several promising attempts to improve the magnetic softness and the GMI effect by stress annealing of Co-rich microwires have been performed [10,51,55].

Generally, stress annealing performed at moderate T_{ann} and σ allows for reduced H_c while the rectangular shape of hysteresis loops is maintained, and even higher M_r/M_0 values are observed.

Several examples are presented below. Similarly to that observed for various Co-rich microwires [47–51], substantial changes in the hysteresis loops are observed after stress annealing. Such changes are affected by several parameters, like T_{ann} and σ. Thus, in Co-rich microwires stress annealed at moderate T_{ann} and σ, lower H_c and higher M_r/M_0 values are observed (see Figure 11). Generally, a decrease in H_c and an increase in M_r/M_0 is observed with increasing σ or T_{ann}. Finally, upon stress annealing at sufficiently high T_{ann} and σ ($T_{ann} = 350\ ^\circ C$; $\sigma = 472$ MPa), the linear hysteresis loop with quite a low magnetic anisotropy field, $H_k \approx 70$ A/m and $H_c \approx 2$ A/m, has been obtained (see Figure 11c).
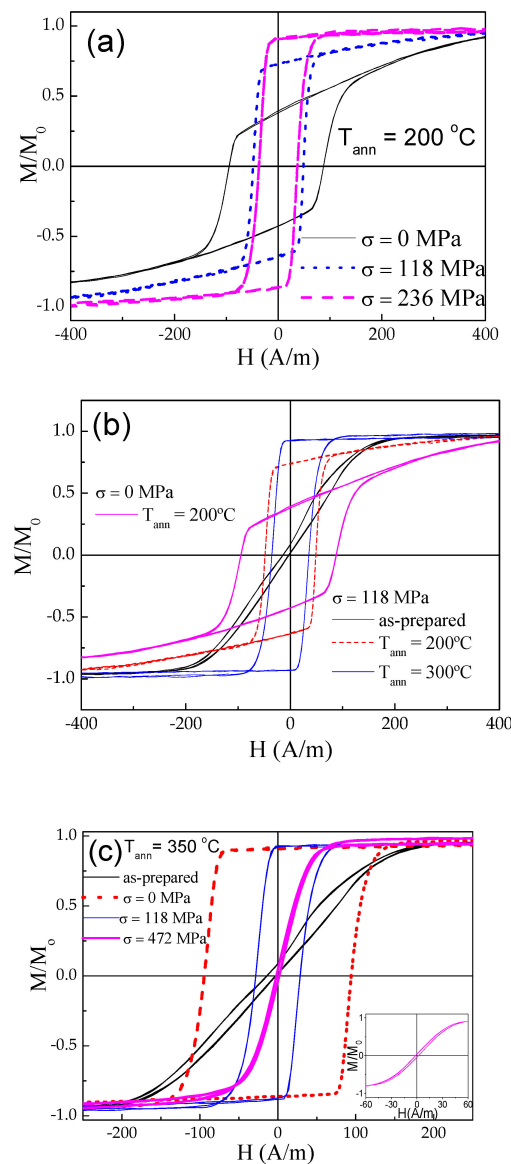
Figure 11. Effects of stress annealing at different conditions on hysteresis loops of $Co_{69.2}Fe_{3.6}Ni_1B_{12.5}Si_{11}C_{1.2}Mo_{1.5}$: effect of σ at $T_{ann} = 200\ ^\circ C$ (**a**), effect of T_{ann} at $\sigma = 118$ MPa (**b**), and effect of σ at $T_{ann} = 350\ ^\circ C$ (**c**), adapted from [55].

Accordingly, a remarkable increase in the GMI ratio is observed in stress-annealed (T_{ann} = 350 °C; σ = 472 MPa) Co-rich microwires as compared to as-prepared Co-rich microwires (see Figure 12). The remarkable increase in $\Delta Z/Z_{max}$ value, as well as the lower H_m value observed in stress-annealed $Co_{69.2}Fe_{3.6}Ni_1B_{12.5}Si_{11}C_{1.2}Mo_{1.5}$ microwires correlate with its better magnetic softness ($H_k \approx 70$ A/m and $H_c \approx 2$ A/m).
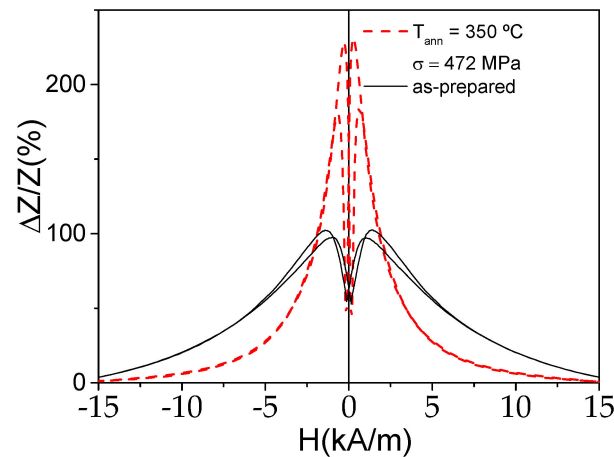

Figure 12. $\Delta Z/Z(H)$ dependencies of as-prepared and stress-annealed (T_{ann} = 350 °C; σ = 472 MPa) $Co_{69.2}Fe_{3.6}Ni_1B_{12.5}Si_{11}C_{1.2}Mo_{1.5}$ microwires measured at f = 100 MHz.

A comparison of $\Delta Z/Z_{max}(f)$ dependencies for as-prepared and stress-annealed samples is provided in Figure 13. For Co-rich samples, the optimum frequency range for the highest $\Delta Z/Z_{max}$ values is about 100–150 MHz. Higher $\Delta Z/Z_{max}$ values for the full frequency range (up to 1 GHz) are observed for stress-annealed Co-rich microwires compared to as-prepared Co-rich microwires. One of the interesting features of stress-annealed Fe-rich samples is the broader frequency range for notable $\Delta Z/Z_{max}$. Additionally, at $f > 500$ MHz, higher $\Delta Z/Z_{max}$ values are obtained for stress-annealed $Fe_{75}B_9Si_{12}C_4$ microwire.
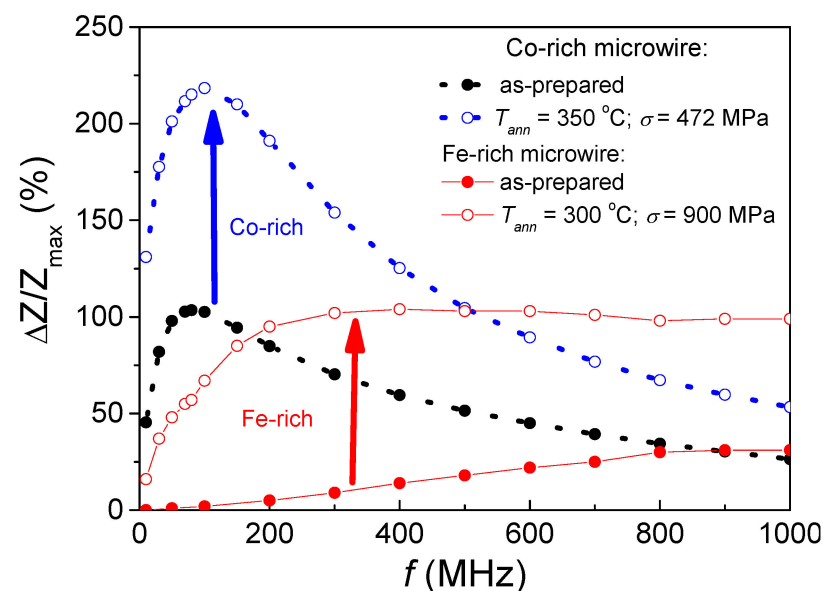

Figure 13. $\Delta Z/Z_{max}(f)$ dependencies for as-prepared and stress-annealed Co-rich and Fe-rich samples.

The origin of magnetic anisotropy induced by stress annealing is either "back stresses" or so-called structural anisotropy or atomic pairs ordering consisting of preferential re-orientation of atomic pairs under the influence of local magnetization [44,56–61]. The

pair atomic ordering mechanism can be relevant for microwires containing two or more ferromagnetic elements. In our case, stress annealing-induced anisotropy is observed for Fe-rich microwires with just one magnetic element.

The aforementioned structural anisotropy originates from a residual bond anisotropy after removing the external stress or from a residual strain [58,62]. In the case of the studied glass-coated microwires, the presence of the glass-coating is associated with strong internal stresses [37,63–65]. Therefore, the influence of such internal stresses can be relevant even during the annealing of the studied glass-coated microwires. Indeed, fine structural rearrangements at the atomic level involving atomic diffusion can be substantially affected by mechanical stresses [65,66].

Previously, the origin of stress-induced anisotropy in Fe-rich amorphous microwires has also been discussed in terms of "back stresses", resulting in a redistribution of the internal stresses after stress annealing [43,44]. Such back stresses have been associated with the slow cooling of glass-coated microwires within the furnace under the applied tensile stress.

As can be observed from Figure 2, both as-prepared and annealed microwires typically present rather similar wide halos. As commonly recognized [61,67], evidence of structural relaxation at the short-range atomic scale in amorphous materials is typically observed through indirect methods. Additionally, common structural methods, like XRD, are mostly useful for topological short-range ordering, i.e., limited to the relative positions of the atoms regardless of their chemical identities [67].

On the other hand, some magnetic properties are quite sensitive to fine changes in the microstructure. Thus, the coercivity, H_c, is among the properties affected by short-range order in the arrangement of atoms [68]. Among the most sensitive magnetic parameters to local structural rearrangements are the Curie temperature, T_c, and the magnetostriction coefficient, λ_s [67,69–71]. Thus, substantial changes in T_c and λ_s reported in various Fe-, Co- and Ni-rich amorphous magnetic materials [67,69–71]. Consequently, considerable modifications in λ_s and T_c are observed in $Co_{67}Fe_{3.85}Ni_{1.45}B_{11.5}Si_{14.5}Mo_{1.7}$ ($\rho \approx 0.96$) microwire after annealing (see Figure 14). Similar influence of annealing on λ_s and T_c observed in various Fe-, Co-, and Ni-rich amorphous alloys were commonly associated with changes in short-range atomic order of amorphous alloys [67,69–71].
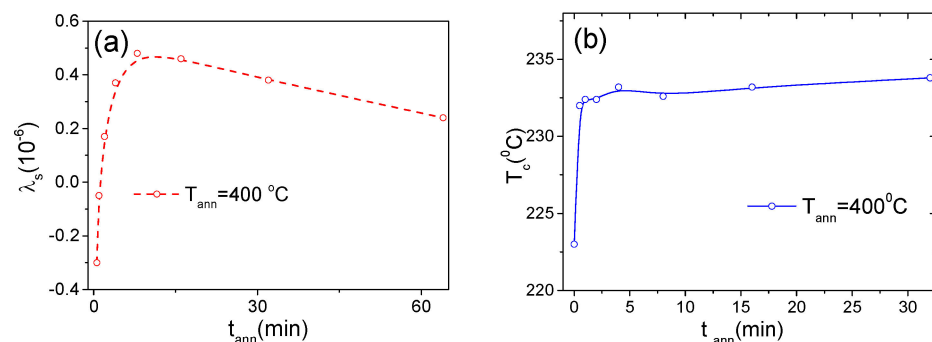

Figure 14. Effect of annealing conditions on λ_s (**a**) and T_c (**b**) of $Co_{67}Fe_{3.85}Ni_{1.45}B_{11.5}Si_{14.5}Mo_{1.7}$ ($\rho \approx 0.96$) microwire. Reproduced with permission from Ref. [71].

Consequently, the origin of the observed changes in magnetic anisotropy, magnetic softness, and the GMI effect in the studied Fe-and Co-rich glass-coated microwires induced either by annealing or by stress annealing can be explained by considering internal stress relaxation, back stresses, or structural magnetic anisotropy.

4. Conclusions

The magnetic softness and GMI effect of both Fe-rich and Co-rich glass-coated microwires can be substantially improved by appropriate postprocessing.

As-prepared Co-rich microwires often present linear hysteresis loops, low coercivity (a few A/m), and a high GMI effect. However, a remarkable magnetic hardening and a transformation of the inclined hysteresis loop into a rectangular loop with a substantial coercivity increase are commonly observed after conventional annealing.

We have demonstrated that stress annealing allows the prevention of magnetic hardening observed after conventional annealing and remarkably improves the GMI effect. Properly stress-annealed Co-rich microwires can present almost unhysteretic loops with low coercivity and magnetic anisotropy field (up to 2 A/m and 70 A/m, respectively).

The observed stress-annealing-induced magnetic anisotropy is affected by the stress-annealing conditions, such as annealing temperature or stresses, applied during annealing. For a given annealing temperature, induced magnetic anisotropy increases with stresses increasing. Similarly, such induced magnetic anisotropy increases with an increase in the annealing temperature at fixed stress.

A remarkable magnetic softening and an order of magnitude increase in the GMI effect is achieved by stress annealing of Fe-rich glass-coated microwires.

Consequently, versatile properties of magnetic microwires (magnetic softness and GMI effect) can be substantially optimized by appropriate postprocessing.

The evaluated frequency dependence of the maximum GMI ratio allows the determination of the optimal GMI measurement conditions for both Fe-rich and Co-rich microwires.

The origin of the observed changes in magnetic anisotropy, soft magnetic properties, and the GMI effect in the studied Fe- and Co-rich glass-coated microwires induced by either annealing or stress annealing has been discussed considering internal stresses relaxation, back stresses, or structural magnetic anisotropy.

Author Contributions: V.Z. and A.Z. designed the concept of the project; V.Z., A.T., A.G., A.G.-G. and P.C.-L. prepared and annealed the samples; M.I., V.Z., J.M.B., P.C.-L. and A.T. performed the magnetic and GMI measurements; A.Z., V.Z. and M.I. participated in the results analysis, discussion, and manuscript preparation; V.Z. and A.Z. obtained the funding. All authors have read and agreed to the published version of the manuscript.

Data Availability Statement: The data presented in this study are available upon request from the corresponding author.

Conflicts of Interest: The authors declare no conflicts of interest.

References

1. Mohri, K.; Humphrey, F.B.; Kawashima, K.; Kimura, K.; Muzutani, M. Large Barkhausen and Matteucci Effects in FeCoSiB, FeCrSiB, and FeNiSiB Amorphous Wires. *IEEE Trans. Magn.* **1990**, *26*, 1789–1791. [CrossRef]
2. Vázquez, M.; Chen, D.-X. The magnetization reversal process in amorphous wires. *IEEE Trans. Magn.* **1995**, *31*, 1229–1239. [CrossRef]
3. Zhukov, A.; Vázquez, M.; Velázquez, J.; Garcia, C.; Valenzuela, R.; Ponomarev, B. Frequency dependence of coercivity in rapidly quenched amorphous materials. *J. Mat. Sci. Eng. A* **1997**, *226–228*, 753–756. [CrossRef]
4. Chen, D.-X.; Dempsey, N.M.; Vázquez, M.; Hernando, A. Propagating domain wall shape and dynamics in iron-rich amorphous wires. *IEEE Trans. Magn.* **1995**, *31*, 781–790. [CrossRef]
5. Panina, L.V.; Mohri, K. Magneto-impedance effect in amorphous wires. *Appl. Phys. Lett.* **1994**, *65*, 1189–1191. [CrossRef]
6. Usov, N.A.; Antonov, A.S.; Lagar'kov, A.N. Theory of giant magneto-impedance effect in amorphous wires with different types of magnetic anisotropy. *J. Magn. Magn. Mater.* **1998**, *185*, 159–173. [CrossRef]

7. Knobel, M.; Vazquez, M.; Kraus, L. Giant magnetoimpedance. In *Handbook of Magnetic Materials*; Bruck, E., Ed.; Elsevier Science Publ. BV: Amsterdam, The Netherlands, 2003; Volume 15, pp. 497–563.

8. Buznikov, N.A. Off-Diagonal Magnetoimpedance in Annealed Amorphous Microwires with Positive Magnetostriction: Effect of External Stresses. *Magnetism* **2023**, *3*, 45–60. [CrossRef]

9. Zhukov, A.; Ipatov, M.; Corte-León, P.; Gonzalez-Legarreta, L.; Churyukanova, M.; Blanco, J.M.; Gonzalez, J.; Taskaev, S.; Hernando, B.; Zhukova, V. Giant magnetoimpedance in rapidly quenched materials. *J. Alloys Compd.* **2020**, *814*, 152225. [CrossRef]

10. Zhukov, A.; Corte-Leon, P.; Gonzalez-Legarreta, L.; Ipatov, M.; Blanco, J.M.; Gonzalez, A.; Zhukova, V. Advanced Functional Magnetic Microwires for Technological Applications. *J. Phys. D Appl. Phys.* **2022**, *55*, 253003. [CrossRef]

11. Honkura, Y.; Honkura, S. The Development of ASIC Type GSR Sensor Driven by GHz Pulse Current. *Sensors* **2020**, *20*, 1023. [CrossRef]

12. Ding, L.; Saez, S.; Dolabdjian, C.; Melo, L.G.C.; Yelon, A.; Ménard, D. Development of a high sensitivity Giant Magneto-Impedance magnetometer: Comparison with a commercial Flux-Gate. *IEEE Sens.* **2009**, *9*, 159–168. [CrossRef]

13. Uchiyama, T.; Mohri, K.; Nakayama, S. Measurement of Spontaneous Oscillatory Magnetic Field of Guinea-Pig Smooth Muscle Preparation Using Pico-Tesla Resolution Amorphous Wire Magneto-Impedance Sensor. *IEEE Trans. Magn.* **2011**, *47*, 3070–3073. [CrossRef]

14. Mohri, K.; Uchiyama, T.; Panina, L.V.; Yamamoto, M.; Bushida, K. Recent Advances of Amorphous Wire CMOS IC Magneto-Impedance Sensors: Innovative High-Performance Micromagnetic Sensor Chip. *J. Sens.* **2015**, *2015*, 718069. [CrossRef]

15. Chiriac, H.; Marinescu, C.S.; Óvári, T.A.; Neagu, M. Sensor applications of amorphous glass-covered wires. *Sens. Actuat. A Phys.* **1999**, *76*, 208–212. [CrossRef]

16. Sabol, R.; Klein, P.; Ryba, T.; Hvizdos, L.; Varga, R.; Rovnak, M.; Sulla, I.; Mudronova, D.; Galik, J.; Polacek, I.; et al. Novel Applications of Bistable Magnetic Microwires. *Acta Phys. Pol. A* **2017**, *131*, 1150–1152. [CrossRef]

17. Hagiwara, M.; Inoue, A.; Masumoto, T. Mechanical properties of Fe–Si–B amorphous wires produced by in-rotating-water spinning method. *Metall. Trans.* **1982**, *13A*, 373–382. [CrossRef]

18. Goto, T.; Nagano, M.; Wehara, N. Mechanical properties of amorphous $Fe_{80}P_{16}C_3B_1$ filament produced by glass-coated melt spinning. *Trans. JIM* **1977**, *18*, 759–764. [CrossRef]

19. Phan, M.H.; Peng, H.X. Giant Magnetoimedance Materials: Fundamentals and Applications. *Prog. Mater. Sci.* **2008**, *53*, 323–420. [CrossRef]

20. Ipatov, M.; Aranda, G.R.; Zhukova, V.; Panina, L.V.; González, J.; Zhukov, A. Tunable effective permittivity of composites based on ferromagnetic microwires with high magneto-impedance effect. *Appl. Phys. A Mater. Sci. Process.* **2011**, *103*, 693–697. [CrossRef]

21. Masumoto, T.; Hashimoto, K. Corrosion properties of amorphous metals. *J. Phys. Colloq.* **1980**, *41*, C8-894–C8-900. [CrossRef]

22. Zhukova, V.; Cobeño, A.F.; Zhukov, A.; de Arellano Lopez, A.R.; López-Pombero, S.; Blanco, J.M.; Larin, V.; Gonzalez, J. Correlation between magnetic and mechanical properties of devitrified glass-coated $Fe_{71.8}Cu_1Nb_{3.1}Si_{15}B_{9.1}$ microwires. *J. Magn. Magn. Mater.* **2002**, *249*, 79–84. [CrossRef]

23. Baranov, S.A.; Larin, V.S.; Torcunov, A.V. Technology, Preparation and Properties of the Cast Glass-Coated Magnetic Microwires. *Crystals* **2017**, *7*, 136. [CrossRef]

24. Chiriac, H.; Lupu, N.; Stoian, G.; Ababei, G.; Corodeanu, S.; Óvári, T.-A. Ultrathin nanocrystalline magnetic wires. *Crystals* **2017**, *7*, 48. [CrossRef]

25. Corte-Leon, P.; Zhukova, V.; Ipatov, M.; Blanco, J.M.; González, J.; Churyukanova, M.; Taskaev, S.; Zhukov, A. The effect of annealing on magnetic properties of "Thick" microwires. *J. Alloys Compd.* **2020**, *831*, 150992. [CrossRef]

26. Ulitovsky, A.V.; Maianski, I.M.; Avramenco, A.I. Method of Continuous Casting of Glass Coated Microwire. Patent No. 128427 (USSR), 15 May 1960. Bulletin No. 10; p. 14.

27. Kraus, L.; Schneider, J.; Wiesner, H. Ferromagnetic resonance in amorphous alloys prepared by rapid quenching from the melt. *Czech. J. Phys. B* **1976**, *26*, 601–602. [CrossRef]

28. Zhukov, A.; Zhukova, V.; Blanco, J.M.; Gonzalez, J. Recent research on magnetic properties of glass-coated microwires. *J. Magn. Magn. Mater.* **2005**, *294*, 182–192. [CrossRef]

29. Pirota, K.R.; Kraus, L.; Chiriac, H.; Knobel, M. Magnetic properties and GMI in a CoFeSiB glass-covered microwire. *J. Magn. Magn. Mater.* **2000**, *21*, L243–L247. [CrossRef]

30. Kronmüller, H.; Fähnle, M.; Domann, M.; Grimm, H.; Grimm, R.; Gröger, B. Magnetic properties of amorphous ferromagnetic alloys. *J. Magn. Magn. Mater.* **1979**, *13*, 53–70. [CrossRef]

31. Kronmüller, H. Theory of the coercive field in amorphous ferromagnetic alloys. *J. Magn. Magn. Mater.* **1981**, *24*, 159–167. [CrossRef]

32. Herzer, G. Amorphous and nanocrystalline soft magnets. In Proceedings of the NATO Advanced Study Institute on Magnetic Hysteresis in Novel Materials, Mykonos, Greece, 1–12 July 1996; NATO ASI Series (Series E: Applied Sciences). Volume 338, pp. 711–730.

33. Konno, Y.; Mohri, K. Magnetostriction measurements for amorphous wires. *IEEE Trans. Magn.* **1989**, *25*, 3623–3625. [CrossRef]

34. Churyukanova, M.; Semenkova, V.; Kaloshkin, S.; Shuvaeva, E.; Gudoshnikov, S.; Zhukova, V.; Shchetinin, I.; Zhukov, A. Magnetostriction investigation of soft magnetic microwires. *Phys. Status Solidi A* **2016**, *213*, 363–367. [CrossRef]

35. Cobeño, A.F.; Zhukov, A.; Blanco, J.M.; Gonzalez, J. Giant magneto-impedance effect in CoMnSiB amorphous microwires. *J. Magn. Magn. Mater.* **2001**, *234*, L359–L365. [CrossRef]

36. Ogasawara, I.; Ueno, S. Preparation and properties of amorphous wires. *IEEE Trans. Magn.* **1995**, *31*, 1219–1223. [CrossRef]
37. Chiriac, H.; Ovari, T.-A. Amorphous glass-covered magnetic wires: Preparation, properties, applications. *Prog. Mater. Sci.* **1996**, *40*, 333–407. [CrossRef]
38. Zhukova, V.; Blanco, J.M.; Ipatov, M.; Gonzalez, J.; Churyukanova, M.; Zhukov, A. Engineering of magnetic softness and giant magnetoimpedance effect in Fe-rich microwires by stress-annealing. *Scr. Mater.* **2018**, *142*, 10–14. [CrossRef]
39. Eggert, R.G. Minerals go critical. *Nat. Chem.* **2011**, *3*, 688–691. [CrossRef]
40. Gonzalez-Legarreta, L.; Corte-Leon, P.; Zhukova, V.; Ipatov, M.; Blanco, J.M.; Gonzalez, J.; Zhukov, A. Optimization of magnetic properties and GMI effect of Thin Co-rich Microwires for GMI Microsensors. *Sensors* **2020**, *20*, 1558. [CrossRef] [PubMed]
41. Zhukov, A.; Ipatov, M.; Corte-Leon, P.; Blanco, J.M.; González-Legarreta, L.; Zhukova, V. Routes for Optimization of Giant Magnetoimpedance Effect in Magnetic Microwires. *IEEE Instrum. Meas. Mag.* **2020**, *23*, 56–63. [CrossRef]
42. Zhukova, V.; Churyukanova, M.; Kaloshkin, S.; Corte-Leon, P.; Ipatov, M.; Zhukov, A. Magnetostriction of amorphous Co-based and Fe-Ni-based magnetic microwires: Effect of stresses and annealing. *J. Alloys Compd.* **2023**, *954*, 170122. [CrossRef]
43. Zhukova, V.; Blanco, J.M.; Corte-Leon, P.; Ipatov, M.; Churyukanova, M.; Taskaev, S.; Zhukov, A. Grading the magnetic anisotropy and engineering the domain wall dynamics in Fe-rich microwires by stress-annealing. *Acta Mater.* **2018**, *155*, 279–285. [CrossRef]
44. Corte-Leon, P.; Zhukova, V.; Blanco, J.M.; Ipatov, M.; Taskaev, S.; Churyukanova, M.; Gonzalez, J.; Zhukov, A. Engineering of magnetic properties and magnetoimpedance effect in Fe-rich microwires by reversible and irreversible stress-annealing anisotropy. *J. Alloys Compd.* **2021**, *855*, 157460. [CrossRef]
45. Buznikov, N.A.; Popov, V.V. A core–shell model for magnetoimpedance in stress-annealed Fe-rich amorphous microwires. *J. Supercond. Nov. Magn.* **2021**, *34*, 169–177. [CrossRef]
46. Nderu, J.N.; Takajo, M.; Yamasaki, J.; Humphrey, F.B. Effect of Stress on Magnetization Process and the Bamboo domains of CoSiB amorphous wires. *IEEE Trans. Magn.* **1998**, *34*, 1312–1314. [CrossRef]
47. Zhukova, V.; Blanco, J.M.; Chizhik, A.A.; Ipatov, M.; Zhukov, A. AC-current-induced magnetization switching in amorphous microwires. *Front. Phys.* **2018**, *13*, 137501. [CrossRef]
48. Popov, V.V.; Buznikov, N.A. Modeling the Giant Magnetoimpedance Effect in Amorphous Microwires with Induced Magnetic Anisotropy. *Phys. Met. Metallogr.* **2020**, *121*, 1033–1038. [CrossRef]
49. Chiriac, H.; Goian, V.; Corodeanu, S. GMI effect in amorphous glass covered microwires as a function of the internal induced stresses. *IEEE Trans. Magn.* **2006**, *42*, 3359–3361. [CrossRef]
50. Zhukov, A.; Talaat, A.; Churyukanova, M.; Kaloshkin, S.; Semenkova, V.; Ipatov, M.; Blanco, J.M.; Zhukova, V. Engineering of magnetic properties and GMI effect in Co-rich amorphous microwires. *J. Alloys Compd.* **2016**, *664*, 235–241. [CrossRef]
51. Gonzalez-Legarreta, L.; Corte-León, P.; Zhukova, V.; Ipatov, M.; Blanco, J.M.; Churyukanova, M.; Taskaev, S.; Zhukov, A. Route of magnetoimpedance and domain walls dynamics optimization in Co-based microwires. *J. Alloys Compd.* **2020**, *830*, 154576. [CrossRef]
52. Vazquez, M.; Gomez-Polo, C.; Chen, D.-X. Switching Mechanism and Domain Structure of Bistable Amorphous Wires. *IEEE Trans. Magn.* **1992**, *28*, 3147–3149. [CrossRef]
53. Barandiaran, M.; Hernando, A.; Madurga, V.; Nielsen, O.V.; Vazquez, M.; Vazquez-Lopez, M. Temperature, stress, and structural-relaxation dependence of the magnetostriction in $(Co_{0.94}Fe_{0.06})_{75}Si_{15}B_{10}$ glasses. *Phys. Rev. B* **1987**, *35*, 5066. [CrossRef]
54. Corte-Leon, P.; Zhukova, V.; Blanco, J.M.; Ipatov, M.; Taskaev, S.; Gonzalez, J.; Zhukov, A. Development of iron-rich microwires with a unique combination of magnetic properties. *Scr. Mater.* **2021**, *195*, 113726. [CrossRef]
55. Zhukov, A.; Gonzalez-Legarreta, L.; Corte-Leon, P.; Ipatov, M.; Maria Blanco, J.; Gonzalez, J.; Zhukova, V. Tailoring of Magnetic Softness and Magnetoimpedance of Co-Rich Microwires by Stress Annealing. *Phys. Status Solidi A* **2021**, *218*, 2100130. [CrossRef]
56. Luborsky, F.E.; Walter, J.L. Magnetic Anneal Anisotropy in Amorphous Alloys. *IEEE Trans. Magn.* **1977**, *13*, 953–956. [CrossRef]
57. Haimovich, J.; Jagielinski, T.; Egami, T. Magnetic and structural effects of anelastic deformation of an amorphous alloy. *J. Appl. Phys.* **1985**, *57*, 3581–3583. [CrossRef]
58. Miyazaki, T.; Takahashi, M. Magnetic annealing effect of amorphous $(Fe_{1-x}Co_x)_{77}Si_{10}B_{13}$ alloys. *J Appl. Phys.* **1978**, *17*, 1755–1763. [CrossRef]
59. Egami, T. Structural relaxation in amorphous $Fe_{40}Ni_{40}P_{14}B_6$ studied by energy dispersive X-ray diffraction. *J. Mater. Sci.* **1978**, *13*, 2587–2599. [CrossRef]
60. Becker, J.J. A new mechanism for magnetic annealing in amorphous metals. *IEEE Tran. Magn.* **1978**, *14*, 938–940. [CrossRef]
61. Ohnuma, M.; Herzer, G.; Kozikowski, P.; Polak, C.; Budinsky, V.; Koppoju, S. Structural anisotropy of amorphous alloys with creep-induced magnetic anisotropy. *Acta Mater.* **2012**, *60*, 1278–1286. [CrossRef]
62. Antonov, A.S.; Borisov, V.T.; Borisov, O.V.; Prokoshin, A.F.; Usov, N.A. Residual quenching stresses in glass-coated amorphous ferromagnetic microwires. *J. Phys. D Appl. Phys.* **2000**, *33*, 1161–1168. [CrossRef]
63. Chiriac, H.; Óvári, T.A.; Pop, G. Internal stress distribution in glass-covered amorphous magnetic wires. *Phys. Rev. B* **1995**, *52*, 10104–10113. [CrossRef]
64. Torcunov, A.V.; Baranov, S.A.; Larin, V.S. The internal stresses dependence of the magnetic properties of cast amorphous microwires covered with glass insulation. *J. Magn. Magn. Mater.* **1999**, *196–197*, 835–836. [CrossRef]
65. Orlova, N.N.; Gornakov, V.S.; Aronin, A.S. Role of internal stresses in the formation of magnetic structure and magnetic properties of iron-based glass coated microwires. *J. Appl. Phys.* **2017**, *121*, 205108. [CrossRef]
66. Onsager, L. Reciprocal Relations in Irreversible Processes. II. *Phys. Rev.* **1931**, *38*, 2265–2279. [CrossRef]

67. Proctor, T.C.; Chudnovsky, E.M.; Garanin, D.A. Scaling of Coercivity in a 3D Random Anisotropy Model. *J. Magn. Magn. Mater.* **2015**, *384*, 181–185. [CrossRef]

68. Egami, T. Structural relaxation in amorphous alloys-compositional short range ordering. *Mat. Res. Bull.* **1978**, *13*, 557–562. [CrossRef]

69. Chen, H.; Sherwood, R.; Leamy, H.; Gyorgy, E. The effect of structural relaxation on the Curie temperature of Fe based metallic glasses. *IEEE Trans. Magn.* **1976**, *12*, 933–935. [CrossRef]

70. Dzhumazoda, A.; Panina, L.V.; Nematov, M.G.; Tabarov, F.S.; Morchenko, A.T.; Bazlov, A.I.; Ukhasov, A.; Yudanov, N.A.; Podgornaya, S.V. Controlling the Curie temperature in amorphous glass coated microwires by heat treatment. *J. Alloys Compd.* **2019**, *802*, 36–40. [CrossRef]

71. Zhukova, V.; García-Gómez, A.; Gonzalez, A.; Churyukanova, M.; Kaloshkin, S.; Corte-Leon, P.; Ipatov, M.; Olivera, J.; Zhukov, A. The Magnetostriction of Amorphous Magnetic Microwires: The Role of the Local Atomic Environment and Internal Stresses Relaxation. *Magnetochemistry* **2023**, *9*, 222. [CrossRef]